Long Range Optical Truck Tracking

Christian Winkens and Dietrich Paulus

University of Koblenz-Landau, Institute for Computational Visualistics, Universitätsstr. 1, 56070 Koblenz, Germany

Keywords: Off-road Platooning, Optical Tracking, Kalman filter, Autonomous Vehicles.

Abstract: Platooning applications require precise knowledge about position and orientation (pose) of the leading vehicle especially in rough terrain. We present an optical solution for a robust pose estimation using artificial markers and a camera as the only sensor. Temporal coherence of image sequences is used in a Kalman filter to obtain precise estimates. Furthermore based on the marker detections we utilize an adaptive model building algorithm which learns a keypoint based representation of the leading vehicle at runtime. The model is continuously updated and allows a markerless tracking of the vehicle for up to 70 meters even when driving at high velocities. The system is designed for and tested in off-road scenarios. A pose evaluation is performed in a simulation testbed.

1 INTRODUCTION AND MOTIVATION

A basic requirement for an intelligent vehicle is the ability to detect and track other vehicles on its path in order to perform platooning, namely, the automatic following of a preceding vehicle. Therefore the so called visual object tracking is an important platooning and computer vision problem which needs to fullfill realtime requirements. One of the main challenges of such a tracking system is the handling of appearance changes of the vehicle during platooning. Appearance changes can be caused varying illumination, out-of-plane rotation and vehicle motion. Put simply, the goal is to localize the target vehicle in a video sequence, given a bounding box that defines the object in an initial frame. Long-term tracking algorithms generally consist of three different modules: a tracker, that estimates object motion, a detector, that localizes the object in the current frame and a learner that updates the object/background model. A variety of approaches have been proposed however they mostly differ in the choice of the object representation, that can include: object silhouette, geometric primitives, points and more. Many proposed algorithms use keypoints for object representation where the main idea is to break down the object into individual parts that are easier to match to a descriptor database than a complete representation of the object. The tracker is initialized by taking the initial bounding box as the source for positive samples and the surrounding as the source for negative samples. One drawback of using keypoints is that due to similar descriptors of object and background elements matching is error-prone and methods like RANSAC are needed to filter outliers.

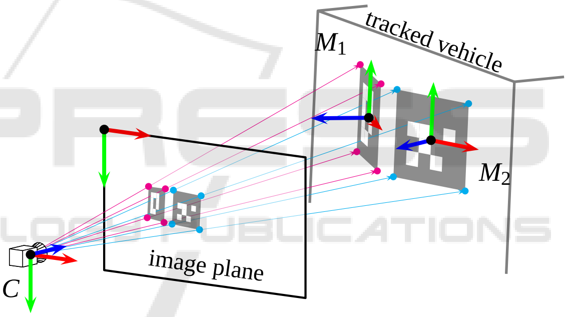

Figure 1: Imaging process $\mathcal{P}$ and measurements used for pose estimation.

The goal of our approach is to allow convoys to move off-roads on rough terrain at relatively high velocities, enabling precise position and orientation estimation even with large distances between leading and following vehicle. In order to solve these problem, we use a mono-camera setup with a high image resolution and artificial markers on the leading vehicle that allows an accurate pose reconstruction and makes use of temporal coherence in order to track the leading vehicle with high precision in a short distance up to 25 meters without any plane-world assumption as proposed in (Winkens et al., 2015). Furthermore we extend this approach and utilize a model learning algorithm which uses the information from the marker

Winkens C. and Paulus D.
Long Range Optical Truck Tracking.
DOI: 10.5220/0006296003300339
In *Proceedings of the 9th International Conference on Agents and Artificial Intelligence (ICAART 2017)*, pages 330-339
ISBN: 978-989-758-220-2

reconstruction to initialize a keypoint based model which is continuously updated and allows a markerless tracking of the vehicle for up to 70 meters even when driving at high velocities or in rough terrain. Our algorithm does not need any prior training or special hardware for processing and relies only on artificial markers for initialization.

This work is structured as follows: Section 2 gives an overview of related work and the pre-requisites for the work presented. Our approach is then introduced (Section 3)). An evaluation is presented in Section 4 and discussed in Section 5.

2 RELATED WORK

Several research topics have to be taken into account when developing an extended pose estimation system that utilizes marker-based and marker-less tracking mechanisms. In the following paragraphs, the relevant state-of-the-art techniques are briefly discussed.

2.1 Platooning

Platooning has already been discussed in many publications. Bergenheim et al. (Bergenhem et al., 2012) provide a good overview to the topic. *Vehicle-To-Infrastructure Communication* (V2I) or *Vehicle-To-Vehicle Communication* (V2V) is utilized by a lot of already published approaches such as (Gehring and Fritz, 1997; Tank and Linnartz, 1997).

Benhimane et al. (Benhimane et al., 2005) use a camera and compute homographies to estimate the pose of a leading vehicle. And Manz et al. (Manz et al., 2011) utilize a particle filter, whereas Franke et al. (Franke et al., 1995) use triangulation.

2.2 Artificial Markers

Artificial markers are of common use, especially in augmented reality (AR) and tracking applications. Various different libraries have been developed and are available free for use (Kato and Billinghurst, 1999; Schmalstieg et al., 2002; Fiala, 2005; Olson, 2011). We decided to use *AprilTags* (Olson, 2011) in our system, to track a leading vehicle and to learn features of it in an initialization phase. AprilTags allow the full 6D localization of features from a single camera image, which allows us a pose reconstruction of an leading vehicle.

2.3 Tracking

The Kalman filter (Kalman, 1960) is of common use in tracking applications. For example, Barth and Franke (Barth and Franke, 2009; Barth and Franke, 2008) proposed a method for image-based tracking of oncoming vehicles from a moving platform using stereo-data and an extended Kalman filter. They used images with a resolution of 640 px by 480 px.

Several surveys (Smeulders et al., 2014; Wu et al., 2015) recently compared tracking performance of several markerless trackers. According to the *Visual Object Tracking challenge* (VOT) (Kristan et al., 2015; Kristan et al., 2016) challenge the top performing trackers applied learned features by convolutional neural nets (CNN), which are quite new to the tracking community. The differences are found in different localisation strategies. Due to the introduction of neural networks huge progress have been made in recent years. The MDNet tracker (Nam et al., 2014) proposed by Nam et al. is trained using a convolutional neural network (CNN) and a set of videos with ground-truth annotations to compute a generic representation of the desired object. The winner of VOT 2016 (Nam et al., 2016) uses multiple collaborating CNNs to track objects in visual sequences. Although trackers based on neural networks deliver very good results, they are mostly too slow, as the results of (Kristan et al., 2015) indicate, to use them in realistic tracking scenarios with real-time requirements right now. Furthermore often special and costly GPUs are needed for the algorithms to work. Usually it's not possible to train an object model a priori, the algorithm must adapt to an object at runtime, which poses a major drawback for CNN based methods which often rely on an a priori training.

Zhu et al. (Zhu et al., 2015) proposed an algorithm which searches in the entire image for informative contours to adapt a generic edge-based objectness measure. Another method using kernel correlation filters using the Fast Fourier Transform (FFT) is presented by Henriques et al. (Henriques et al., 2015), which achieves good performance but cannot handle the occlusion problem well. An real-time capable algorithm is presented by Henriques et al. (Hare et al., 2011), which extends an online structured output SVM learning method, which is learned online, to suit the tracking problem. Unfortunately Struck does not handle scale variation, which is a major problem in our scenario where large scale variations appear. Another approach is to build models on the distinction of the target against background by using point features like BRISK (Leutenegger et al., 2011), FREAK (Ortiz, 2012) or ORB (Rublee et al., 2011).

Examples are proposed by Maresca et al. (Maresca and Petrosino, 2013) and Nebehay et al. (Nebehay and Pflugfelder, 2015). Nebehay uses BRISK features and a static model in a combined matching and tracking framework and a consensus-based clustering for outlier detection. Maresca however uses multiple key point-based features together in combination with a learning module which updates the object model, utilizing a growing and pruning approach. Here the use of multiple features sacrifices speed for improved robustness. As (Wu et al., 2015) stated, the use of a motion or a dynamic model is crucial for robust object tracking, but the most evaluated trackers do not incorporate such components. Altough it could speed up and improve robustness and efficiency. An active appearance model is used by Matthews et al. (Matthews et al., 2004) to update models in an visual tracking scenario.

3 OPTICAL TRACKING APPROACH

In our setup we use a high resolution camera, which is mounted on a vehicle that pursues a leading vehicle. Two static artificial markers are mounted at the back of the leading vehicle. This marker setup is observed by the camera mounted on the following vehicle. Obeserving the marker setup, our systems is ablew to reconstruct the pose of the leading vehicle at ranges up to 25 m and at the same time we learn a model of the vehicle, so that a tracking of the vehicle is possible when the markers can no longer reconstructed because of a great distance from the preceding vehicle. Furthermore, the learned model is used to increase the stability of pose reconstruction done by the Kalman filter in the close range.

Figure 2 and Figure 3 illustrate the geometric setup of the camera and the markers and define the coordinate systems used in our system:

Symbol	Coordinate System
C	Camera
T	Following Vehicle
M_i	Marker M_i
V	Leading Vehicle

A *pose* is defined as the position and orientation of an object in *3-D* space. It is defined as a tuple $p = \langle s, q \rangle$ with $s \in \mathbb{R}^3$ the position of the object relative to the origin of the coordinate system and $q \in \mathbb{R}^4$ the vector representation of a unit quaternion for the rotation relative to the coordinate system's orthonormal bases.

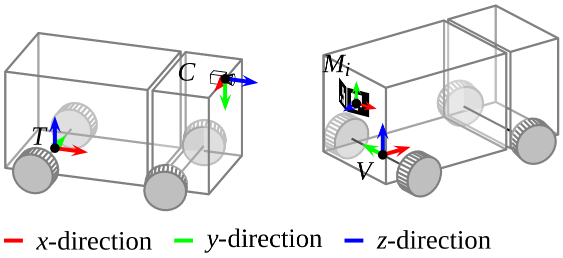

Figure 2: Defined coordinate systems and orientation of the orthonormal bases.

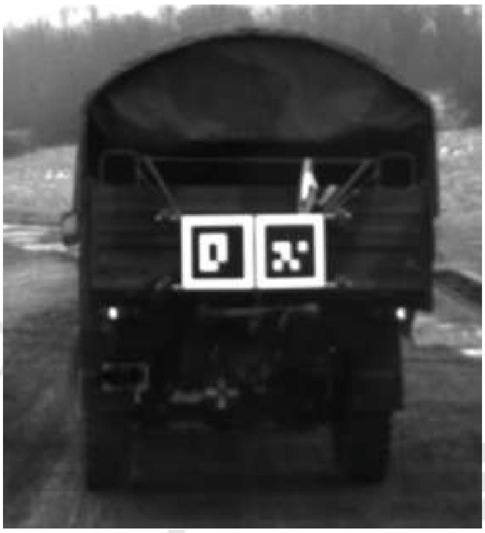

Figure 3: Artificial marker mounted on leading vehicle.

Our system can deal with various marker setups and configurations, but at least one marker is required for our method to work. The precision of the pose estimation will increase with higher numbers of (visible) markers.

In our setup, two artificial markers are mounted on the back of the leading vehicle. They are slightly rotated in order to be viewable from the side as well (see Figure 3).

3.1 Kalman Filter

As the estimation of the pose of the leading vehicle is prone to uncertainties, a Kalman filter (Kalman, 1960) is utilized to improve the pose estimate. The dynamic Kalman state of the vehicle pose is represented by a vector:

$$x = \left(s^{\mathrm{T}}, q^{\mathrm{T}}, v^{\mathrm{T}}, \omega^{\mathrm{T}}\right)^{\mathrm{T}} \in \mathbb{R}^{13}.$$

Where $s = (s_x, s_y, s_z)^{\mathrm{T}}$ the position and $q \in \mathbb{R}^4, q = (q_w, q_x, q_y, q_z)^{\mathrm{T}}$, the vector representation of a unit quaternion, define the position and orientation of the leading vehicle relative to the following vehicle. The vectors $v \in \mathbb{R}^3$ and $\omega \in \mathbb{R}^3$ describe the system's linear and angular velocity. For more details on our kalman tracking system please refer to (Winkens et al., 2015).

3.2 (Re-)Initialization

At first our system searches for our marker-system in the given camera image. If visible the mounted markers are detected by our tracking system and a Kalman filter is initialized. The pose of the leading vehicle is tracked using the Kalman filter using a linear motion model. A good initial value of the pose p in the dynamic state x is vital for proper estimation. When launching the pose estimation process, pose p is initialized by solving the point correspondence problem using the raw marker corner detections. If the algorithm is not able to detect markers over a certain time, it will fall back to the initialization mode.

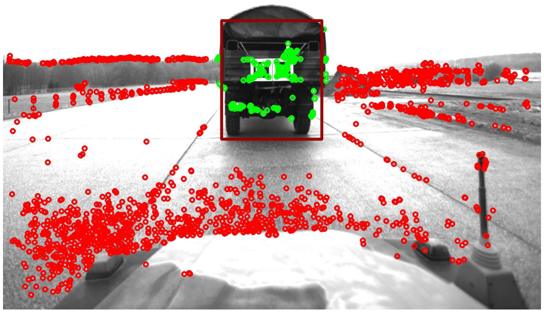

Figure 4: Initialization of markerless tracker with K_0 as nodel points (green) and B_0 as background points (red).

3.3 Markerless Tracking

The maximum possible tracking range is directly limited by marker size and camera resolution. In order to increase the range of the existing tracking system, it is necessary not only to detect the markers and track them, but to use the size of the vehicle and track the vehicle itself. This requires to learn an abstracted model of the vehicle, which is then used to track the vehicle in each new frame of the data stream. As with other trackers, the problem is then reduced to determine a bounding box enclosing the object, in each frame. Our markerless tracking system is initialized with the reconstructed pose and an initial bounding box b_0 provided by the Kalman filter. The algorithm then calculates keypoints $\kappa_1^0, \ldots, \kappa_l^0$ on the initial frame F_0 and splits them in object points $K_0 = \{\kappa_1^0, \ldots, \kappa_l^0\}$ and background points $B_0 = \{\kappa_1^0, \ldots, \kappa_n^0\}$ by using the supported bounding box as illustrated in Figure 4. Based on this bounding box we calculate ORB features and store them in two separate models for each element of the two sets of points. In addition, the center of the bounding box and the pairwise distances between the feature locations is calculated and stored. Furthermore, the object points are normalized by the relative position of the feature points to the bounding box center. After receiving the next frame F_t the marker-based (Kalman filter) tracking first tries to reconstruct a pose using the detected marker corners. In a second step the markerless tracking tries to locate the desired object in the picture. A naive approach would be to calculate the features throughout the frame F_t and search for correspondences with the object model. However, since the feature calculation on a full resolution image would be very time consuming the search space must be restricted to meet real-time requirements. The initial object model points are used to calculate the optical flow (yves Bouguet, 2000) between the two frames:

$$\kappa_1(x,y,t) = \kappa_1(x+dx, y+dy, 0+dt) \tag{1}$$

By utilizing optical flow a potential region of interest can be estimated, which is expanded by a certain factor to account for uncertainties. This bounding box defines a subregion F_t^p of the frame, which is taken to compute the features. The features $\{\kappa_1^t, \ldots, \kappa_n^t\} \in F_t$ are now matched against a model consisting of object and background features. To prevent from false correspondences between the model and candidates all features that correlate with background features are directly discarded from the matching process. The rest is matched utilizing the distance ratio method (Lowe, 2004) to filter false positives. The correspondences thus found now give the set of Υ_t^+. After that the matched correspondences using optical flow estimation and global matching are fused, wherein the optical flow matches overrule the global matching. Using the matched features we estimate scale s and rotation α as proposed by (Kalal et al., 2010) and (Nebehay and Pflugfelder, 2014).

$$s = \mathrm{med}\left(\left\{\frac{||\kappa_i^t - \kappa_j^t||}{||\kappa_i^0 - \kappa_j^0||}, i \neq j\right\}\right) \tag{2}$$

$$\alpha = \mathrm{med}(\{\mathrm{atan}(\kappa_i^0 - \kappa_j^0) - \mathrm{atan}(\kappa_i^t - \kappa_j^t), i \neq j\}) \tag{3}$$

A static appearance model is used, which is based on the initial appearance of the object, composed of the initial descriptors K_0. The model can not adapt to appearance changes of the object or the background. This is in the present scenario particularly relevant as very large changes occur in the scaling of the object, also the background can underly massive changes. To account for this, the background model is adapted periodically to account for changes in the environment. Features from the background database are picked randomly and replaced by features from the current frame, which do not intersect with the detected object. Furthermore a homography is estimated based on the matched features using the RANSAC method (Fischler and Bolles, 1981). Correspondences which do not correspond to the calculated homography are sorted out as outliers. Thus, a correct data association, which is essential for the reconstruction of the points, can be achieved.

3.4 Feature Pose Reconstruction

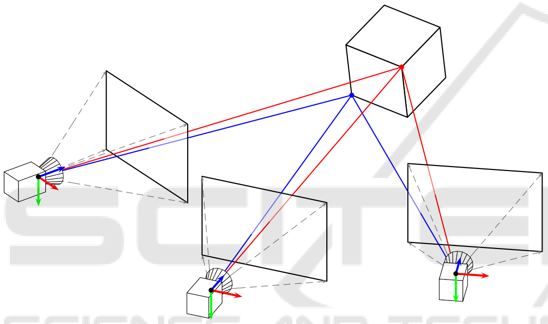

Figure 5: Shematic description of our feature pose reconstruction approach.

To support the marker based pose estimation, we use features from the previously learned object model, as described previously in 3.3. We try to estimate the 3-D position of these points, relative to the origin of the preceding vehicle by accounting different observations of the feature in different frames during tracking, as illustrated by Figure 5. Knowing the 3-D position of the these feature points we could use their observations in new frames to update the Kalman filter and support marker-based tracking.

The observation of a feature $\mathbf{d_{ij}}$ which is seen from camera pose $\mathbf{c}_i$ can be expressed as an measurement in the form:

$$\mathbf{h}(\mathbf{m}_j, \mathbf{c}_i) = \mathcal{P}(\mathcal{T}(\mathbf{c}_i)^{-1} \cdot \mathbf{m}_j) \tag{4}$$

Where $\mathcal{P}$ denotes the intrinsic camera model and $\mathcal{T}(\mathbf{c}_i)^{-1}$ describes the transformation of the feature points in the coordinate system of the camera. Using this prediction function the total back projection error over alle features can now denoted as:

$$\underset{\mathbf{m}_*, \mathbf{c}_*}{\operatorname{argmin}} \sum_i \sum_j ||\mathbf{h}(\mathbf{m}_j, \mathbf{c}_i) - \mathbf{d}_{ij}||^2 \tag{5}$$

Which defines the sum of all differences between the predicted $\mathbf{h}(.,.)$ and the actually observed positions of feature $\mathbf{d}_{ij}$. The minimum represents the optimum utilization of all 3D feature positions and camera poses. The optimization of this non-linear least-squares problem is solved using the library *Ceres* (Agarwal et al.,). The basic prerequisite for the bundle adjustment described above is the robust tracking of feature points from different camera views. Since feature tracking is never perfect, the system must be able to deal with outliers, or mistracked points. For this reason, we use a robust loss function which limits the influence of coarse outliers and effectively prevents individual wrong tracked features from misleading the reconstruction.

Equation 5 is non-linear and non-convex. As a result, the convergence of the optimization process to the correct solution strongly depends on initialization parameters. We take the initialization of the camera poses from the marker-based tracking and initialize the feature locations in the origin of the preceding vehicle. Simultaneously, a prior is set on the feature locations, which expresses a low certainty that the feature lies in the vicinity of the origin of the preceding vehicle. This is useful to limit the uncertainty in z-direction especially in the case of only a few observations with low baseline.

The used artificial markers are visible in nearly all camera frames, which are used to reconstruct the features and the corners of these markers can be seen as normal feature points. But their position in the coordinate system is fixed and known to our system, so we use them to enhance the reconstruction because *Ceres* allows selective fixing of parameters during optimization. Therefore we add the corner points to the optimization problem and declared them as fixed. The fixed corner points also define the scale of the optimized points that could not be determined without such a metric reference.

Solving this system of equations is computationally intensive and requires much time. Each new frame provides, according to the correspondences found, new terms to the optimization problem, which will bloat the system of equations in a short period of time. Furthermore provide frames which are temporally close to each other little new information, since the spatial distance between them is very low. Also note that great distances between camera and vehicle lead to worse results in feature matching and tracking. Because the risk of false correspondences heavily correlates with increasing distance.

Therefore we ensure that only information from camera poses with a euclidean distance of 0.2 m and more to the others is added to the system. In addition, only camera poses are added, which are below a distance of 20 m to the vehicle driving ahead to minimize risk of false correspondences.

Due to the automatic initialization of the markerless tracking it is possible that features are used, which do not belong to the vehicle or are very weak. This may distract the tracking system in the long run because it raises the chance of false correspondences. Therefore, a model management has been integrated, which periodically checks the quality of the model and exchanges weak features. We calculate the reprojection error of all reconstructed feature positions with respect to all reconstructed poses and take the mean. In a second step all features with an reprojection error greater than the mean are removed from the model and new features are added instead.

3.5 Pose estimation

The learned and 3-D reconstructed model points are additionally used by the Kalman filter at runtime to improve the pose estimation. For this purpose, the observations $\mathbf{z}_k$ of the reconstructed keypoints $\mathbf{m}_j$ are used as measurements for additional kalman update steps. Observations are predicted similar to the marker corner points using the measurement model:

$$\hat{\mathbf{z}}_k = \mathcal{P}(\mathcal{T}_{T\to C} \cdot \mathcal{T}_{V\to T}(\mathbf{p}_k, \mathbf{q}_k) \cdot m_j) + \mathbf{g}_k \qquad (6)$$

The two-dimensional random variable $\mathbf{g}_k \sim \mathcal{N}(\mathbf{0}, \mathbf{R}_k)$ models the measuring noise, which is assumed here as 1 px in the *u*- or *v*-direction.

The measurement model transforms the model point m_j using the $\mathbf{p}_k, \mathbf{q}_k$ from the dynamic system state $\mathbf{x}_k$ of the Kalman filter into the coordinate system of the following vehicle. Using the known position of the camera in the rear-running vehicle, the point is transformed into the camera coordinate system C. The function $\mathcal{P}$ performs a projection onto the image plane as well as the radial distortion of the point, just as before applying the known intrinsic calibration of the camera. The described Kalman update step is executed exactly once for the model points observed in the current frame. The remaining procedure of the Kalman filter remains unchanged.

4 EVALUATION

The system is designed to work at high velocities and in off-road scenarios. Therefore capturing ground truth data for evaluation is a difficult issue, as a high precision in the pose of both the following and the leading vehicle is mandatory. External position tracking systems do not suit the demands as the required off-road track is too long and it is therefore too cost- and time-intense to equip with appropriate hardware. Standaerd radio based position systems such as GPS or Galileo do not offer an adequate pose quality. Equipping one of the vehicles with hardware like *3-D* LIDAR sensors does not present a solution as well, because the sensors themselves have uncertainties. To make things worse, we consider an off-road scenario where a full *6-D* pose is required as a ground truth.

4.1 Evaluation using Synthetic Camera Images

Our approach for evaluation of the marker-based tracking is based on a virtual testbed. A simulation environment is utilized for the generation of synthetic camera images: The simulation environment used is derived from published approaches for pose estimate evaluations (Fuchs et al., 2014b; Fuchs et al., 2014a) using synthetic images. Its adaptive architecture allows an easy integration. The camera in the simulation environment can be configured to match various resolutions and opening angles to test the impact on the pose quality. The intrinsic camera parameters needed for the pose tracking can easily be derived from the simulation configuration following the method described by Fuchs et al. (Fuchs et al., 2014b). The evaluation results of our marker-based tracking system were proposed previously in (Winkens et al., 2015). A distance measurement defined by Park (Park, 1995) was used and discussed by Huynh (Huynh, 2009):

$$\Gamma(q, q') = \| \log(\Phi(q), \Phi(q')^{\mathrm{T}}) \|$$

Where $\Phi : \mathbb{R}^4 \to \mathbb{R}^{3\times 3}$ converts a quaternion to a rotation matrix. In a first evaluation, the rendered image sequences have directly been processed the Kalman tracking as proposed above. In a second pass, Gaussian noise $\mathcal{N}(0, I_{2\times 2})$ was added to the raw marker detections extracted from the image. This way, we were able to quantify the robustness of our method using noisy data. The synthetic tests, as published in (Winkens et al., 2015) show that the tracking system has a translation error of $7,3$ cm at a distance of 8 m.The average error in the orientation (avg $|\Gamma|$) is 0.06 Rad ≈ 3.4 Deg proving the robustness and precision of the system proposed.

4.2 Off-road Testing Scenario

Evaluation of the marker-free tracking extension for long range outdoor tracking is difficult, as these synthetic tests are not applicable. A good evaluation

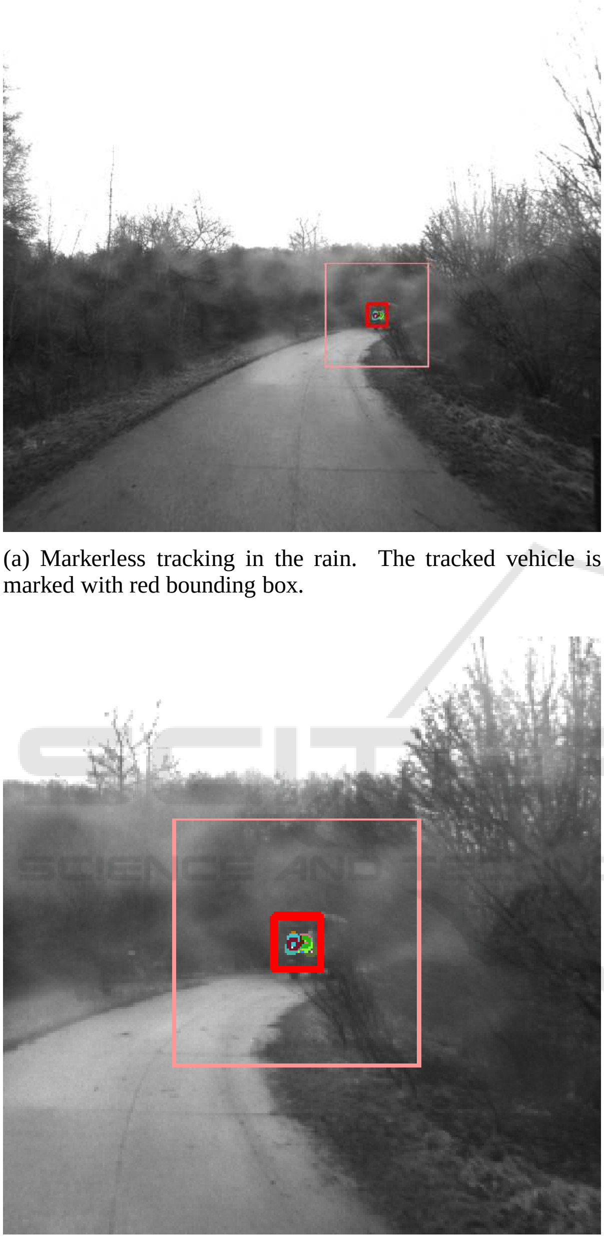

(a) Markerless tracking in the rain. The tracked vehicle is marked with red bounding box.

(b) Magnified version, with tracked vehicle in red bounding-box and matched features (colored circles).

Figure 6: Visualization of our long range markerless tracking during rain.

would require two Real Time Kinematic (RTK) systems mounted on both vehicles. Unfortunately, we do not own such a system, but we plan to equip our vehicles with it in the near future. Therefore pose estimation system as proposed in this publication has been tested and evaluated using datasets specif-

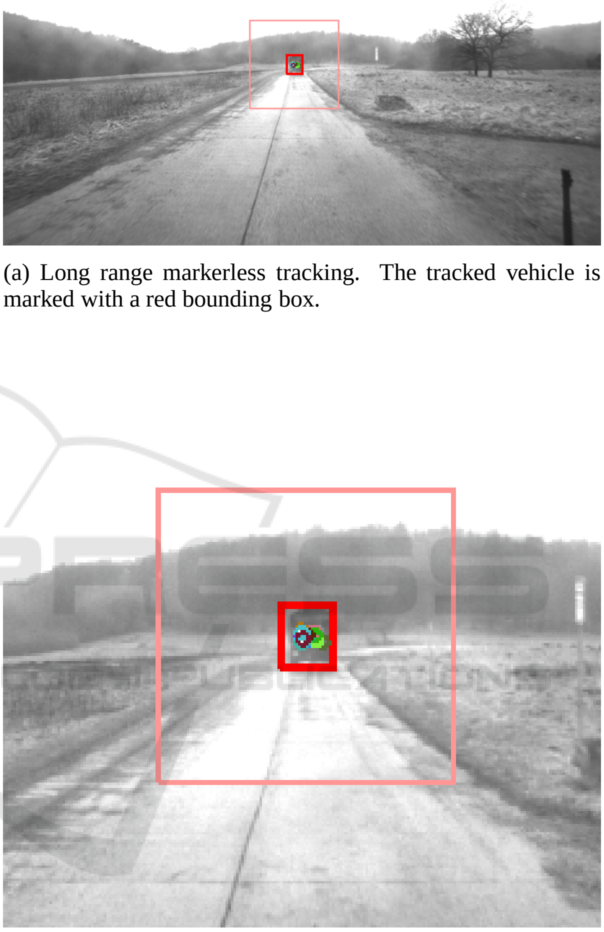

(a) Long range markerless tracking. The tracked vehicle is marked with a red bounding box.

(b) Magnified version of the above image with matched features from object model (colored circles).

Figure 7: Visualization of our long range markerless tracking.

ically recorded for this purpose with velocities up to 60 km/h. A truck with a artificial marker system mounted on its back was followed by another vehicle equipped with a high resolution camera. The recorded data is used as the input for our system and is processed in realtime. The vehicle tracked by our tracking system is highlighted with a red bounding-box in the camera images, facilitating a visual examination of our results in Figure 6 and Figure 7. Additionally we provide a video which can be viewed here[1]. The examination showed that the system provided a robust tracking up to a range of 70 m while processing at 10 to 15 Hz on standard mobile-computer hardware. However, a quantitative analysis of the system cannot be done in this scenario, because no reliable ground truth pose information is available. Together with this work we provide a video, which allows the visual evaluation of the quality of the tracker.

5 CONCLUSION

We proposed an extended optical tracking mechanism that only uses one camera and artificial markers to track a vehicle driving at high velocities and great distances. A Kalman filter is utilized to include the advantages of temporal coherence. Our system is able of estimating the relative pose between two vehicles in real-time up to 26 m and tracking the vehicle itself within a range up to 70 m. At an average distance of 8 m, the average absolute of the Kalman filter error in the translation, including artificial noise, ($\text{avg}\,|\Delta|$) is about $7.3\,\text{cm}$ with an average error in the orientation of($\text{avg}\,|\Gamma|$) $0.06\,\text{Rad} \approx 3.4\,\text{Deg}$.

With the pose estimation and markerless tracking proposed, we introduced an algorithm capable of tracking leading vehicles in off-road platooning scenarios, without the need for communication and/or infrastructure. The leading vehicle could therefore be a regular truck equipped with a marker pattern. This saves time and reduces costs significantly, as no complex setup is necessary. The system works independently from any external services and infrastructure. The proposed system learns a model by detecting features on the leading vehicle at runtime, so that the pose of the vehicle can still be estimated even when the leading vehicle gets too far away to detect the artificial markers. In closer range scenarios, dynamic features improve the accuracy of the estimated pose. We will further investigate the use of a second camera to enhance tracking and pose estimation precision. Furthermore we will equip our vehicles with some RTK systems to provide a ground truth and allow a proper evaluation in the near future.

ACKNOWLEDGEMENTS

This work was partially funded by Wehrtechnische Dienststelle 41 (WTD), Koblenz, Germany.

[1] https://www.dropbox.com/s/ly15h24085uyggp/longrangetracking.mp4

REFERENCES

Agarwal, S., Mierle, K., and Others. Ceres solver.

Barth, A. and Franke, U. (2008). Where will the oncoming vehicle be the next second? In *IEEE Intelligent Vehicles Symposium*, pages 1068–1073.

Barth, A. and Franke, U. (2009). Estimating the driving state of oncoming vehicles from a moving platform using stereo vision. *IEEE Transactions on Intelligent Transportation Systems*, 10(4):560–571.

Benhimane, S., Malis, E., Rives, P., and Azinheira, J. (2005). Vision-based control for car platooning using homography decomposition. In *IEEE International Conference on Robotics and Automation*, pages 2161–2166.

Bergenhem, C., Shladover, S., Coelingh, E., Englund, C., and Tsugawa, S. (2012). Overview of platooning systems. In *Proceedings of the 19th ITS World Congress, Vienna*.

Fiala, M. (2005). Artag, a fiducial marker system using digital techniques. In *IEEE Computer Society Conference on Computer Vision and Pattern Recognition*, volume 2, pages 590–596. IEEE.

Fischler, M. A. and Bolles, R. C. (1981). Random sample consensus: a paradigm for model fitting with applications to image analysis and automated cartography. *Communications of the ACM*, 24(6):381–395.

Franke, U., Bottiger, F., Zomotor, Z., and Seeberger, D. (1995). Truck platooning in mixed traffic. In *IEEE Intelligent Vehicles Symposium*, pages 1–6.

Fuchs, C., Eggert, S., Knopp, B., and Zöbel, D. (2014a). Pose detection in truck and trailer combinations for advanced driver assistance systems. In *IEEE Intelligent Vehicles Symposium Proceedings*, pages 1175–1180. IEEE.

Fuchs, C., Zöbel, D., and Paulus, D. (2014b). 3-d pose detection for articulated vehicles. In *13th International Conference on Intelligent Autonomous Systems (IAS)*.

Gehring, O. and Fritz, H. (1997). Practical results of a longitudinal control concept for truck platooning with vehicle to vehicle communication. In *IEEE Conference on Intelligent Transportation System (ITSC)*, pages 117–122.

Hare, S., Saffari, A., and Torr, P. H. (2011). Struck: Structured output tracking with kernels. In *Computer Vision (ICCV), 2011 IEEE International Conference on*, pages 263–270. IEEE.

Henriques, J. F., Caseiro, R., Martins, P., and Batista, J. (2015). High-speed tracking with kernelized correlation filters. *Pattern Analysis and Machine Intelligence, IEEE Transactions on*, 37(3):583–596.

Huynh, D. (2009). Metrics for 3d rotations: Comparison and analysis. *Journal of Mathematical Imaging and Vision*, 35(2):155–164.

Kalal, Z., Mikolajczyk, K., and Matas, J. (2010). Forward-backward error: Automatic detection of tracking failures. In *In Proceedings of the 2010 20th International Conference on Pattern Recognition, ICPR 10*, pages 2756–2759. IEEE Computer Society.

Kalman, R. E. (1960). A new approach to linear filtering and prediction problems. *Journal of Fluids Engineering*, 82(1):35–45.

Kato, H. and Billinghurst, M. (1999). Marker tracking and hmd calibration for a video-based augmented reality conferencing system. In *2nd IEEE and ACM International Workshop on Augmented Reality. (IWAR'99) Proceedings.*, pages 85–94. IEEE.

Kristan, M., Leonardis, A., Matas, J., Felsberg, M., Pflugfelder, R., Čehovin, L., Vojír, T., Häger, G., Lukežič, A., Fernández, G., Gupta, A., Petrosino, A., Memarmoghadam, A., Garcia-Martin, A., Solís Montero, A., Vedaldi, A., Robinson, A., Ma, A. J., Varfolomieiev, A., Alatan, A., Erdem, A., Ghanem, B., Liu, B., Han, B., Martinez, B., Chang, C.-M., Xu, C., Sun, C., Kim, D., Chen, D., Du, D., Mishra, D., Yeung, D.-Y., Gundogdu, E., Erdem, E., Khan, F., Porikli, F., Zhao, F., Bunyak, F., Battistone, F., Zhu, G., Roffo, G., Subrahmanyam, G. R. K. S., Bastos, G., Seetharaman, G., Medeiros, H., Li, H., Qi, H., Bischof, H., Possegger, H., Lu, H., Lee, H., Nam, H., Chang, H. J., Drummond, I., Valmadre, J., Jeong, J.-c., Cho, J.-i., Lee, J.-Y., Zhu, J., Feng, J., Gao, J., Choi, J. Y., Xiao, J., Kim, J.-W., Jeong, J., Henriques, J. F., Lang, J., Choi, J., Martinez, J. M., Xing, J., Gao, J., Palaniappan, K., Lebeda, K., Gao, K., Mikolajczyk, K., Qin, L., Wang, L., Wen, L., Bertinetto, L., Rapuru, M. K., Poostchi, M., Maresca, M., Danelljan, M., Mueller, M., Zhang, M., Arens, M., Valstar, M., Tang, M., Baek, M., Khan, M. H., Wang, N., Fan, N., Al-Shakarji, N., Miksik, O., Akin, O., Moallem, P., Senna, P., Torr, P. H. S., Yuen, P. C., Huang, Q., Martin-Nieto, R., Pelapur, R., Bowden, R., Laganière, R., Stolkin, R., Walsh, R., Krah, S. B., Li, S., Zhang, S., Yao, S., Hadfield, S., Melzi, S., Lyu, S., Li, S., Becker, S., Golodetz, S., Kakanuru, S., Choi, S., Hu, T., Mauthner, T., Zhang, T., Pridmore, T., Santopietro, V., Hu, W., Li, W., Hübner, W., Lan, X., Wang, X., Li, X., Li, Y., Demiris, Y., Wang, Y., Qi, Y., Yuan, Z., Cai, Z., Xu, Z., He, Z., and Chi, Z. (2016). *The Visual Object Tracking VOT2016 Challenge Results*, pages 777–823. Springer International Publishing.

Kristan, M., Matas, J., Leonardis, A., Felsberg, M., Čehovin, L., Fernandez, G., Vojir, T., Häger, G., Nebehay, G., Pflugfelder, R., Gupta, A., Bibi, A., Lukežič, A., Garcia-Martin, A., Saffari, A., Petrosino, A., Montero, A. S., Varfolomieiev, A., Baskurt, A., Zhao, B., Ghanem, B., Martinez, B., Lee, B., Han, B., Wang, C., Garcia, C., Zhang, C., Schmid, C., Tao, D., Kim, D., Huang, D., Prokhorov, D., Du, D., Yeung, D.-Y., Ribeiro, E., Khan, F. S., Porikli, F., Bunyak, F., Zhu, G., Seetharaman, G., Kieritz, H., Yau, H. T., Li, H., Qi, H., Bischof, H., Possegger, H., Lee, H., Nam, H., Bogun, I., chan Jeong, J., il Cho, J., Lee, J.-Y., Zhu, J., Shi, J., Li, J., Jia, J., Feng, J., Gao, J., Choi, J. Y., Kim, J.-W., Lang, J., Martinez, J. M., Choi, J., Xing, J., Xue, K., Palaniappan, K., Lebeda, K., Alahari, K., Gao, K., Yun, K., Wong, K. H., Luo, L., Ma, L., Ke, L., Wen, L., Bertinetto, L., Pootschi, M., Maresca, M., Danelljan, M., Wen, M., Zhang, M., Arens, M., Valstar, M., Tang, M., Chang, M.-C., Khan, M. H., Fan, N., Wang, N., Miksik, O., Torr, P. H. S., Wang, Q., Martin-Nieto, R., Pelapur, R., Bowden, R., Laganiere, R., Moujtahid, S., Hare, S., Hadfield, S., Lyu, S., Li, S., Zhu, S.-C., Becker, S., Duffner, S., Hicks, S. L., Golodetz, S., Choi, S., Wu, T., Mauthner, T., Pridmore, T., Hu, W., Hübner, W., Wang, X., Li, X., Shi, X., Zhao, X., Mei, X., Shizeng, Y., Hua, Y., Li, Y., Lu, Y., Li, Y., Chen, Z., Huang, Z., Chen, Z., Zhang, Z., and He, Z. (2015). The visual object tracking vot2015 challenge results.

Leutenegger, S., Chli, M., and Siegwart, R. Y. (2011). Brisk: Binary robust invariant scalable keypoints. In *Proceedings of the 2011 International Conference on Computer Vision*, ICCV '11, pages 2548–2555, Washington, DC, USA. IEEE Computer Society.

Lowe, D. G. (2004). Distinctive image features from scale-invariant keypoints. *International Journal of Computer Vision*, 60:91–110.

Manz, M., Luettel, T., von Hundelshausen, F., and Wuensche, H.-J. (2011). Monocular model-based 3d vehicle tracking for autonomous vehicles in unstructured environment. In *IEEE International Conference on Robotics and Automation (ICRA)*, pages 2465–2471.

Maresca, M. E. and Petrosino, A. (2013). *Image Analysis and Processing – ICIAP 2013: 17th International Conference, Naples, Italy, September 9-13, 2013, Proceedings, Part II*, chapter MATRIOSKA: A Multi-level Approach to Fast Tracking by Learning, pages 419–428. Springer Berlin Heidelberg, Berlin, Heidelberg.

Matthews, I., Ishikawa, T., and Baker, S. (2004). The template update problem. *IEEE Transactions on Pattern Analysis & Machine Intelligence*, (6):810–815.

Nam, H., Baek, M., and Han, B. (2016). Modeling and propagating cnns in a tree structure for visual tracking. *arXiv preprint arXiv:1608.07242*.

Nam, H., Hong, S., and Han, B. (2014). Online graph-based tracking. In *Computer Vision–ECCV 2014*, pages 112–126. Springer.

Nebehay, G. and Pflugfelder, R. (2014). Consensus-based matching and tracking of keypoints for object tracking. In *Applications of Computer Vision (WACV), 2014 IEEE Winter Conference on*, pages 862–869. IEEE.

Nebehay, G. and Pflugfelder, R. (2015). Clustering of Static-Adaptive correspondences for deformable object tracking. In *Computer Vision and Pattern Recognition*. IEEE.

Olson, E. (2011). AprilTag: A robust and flexible visual fiducial system. In *2011 IEEE International Conference on Robotics and Automation (ICRA)*, pages 3400–3407. IEEE.

Ortiz, R. (2012). Freak: Fast retina keypoint. In *Proceedings of the 2012 IEEE Conference on Computer Vision and Pattern Recognition (CVPR)*, CVPR '12, pages 510–517, Washington, DC, USA. IEEE Computer Society.

Park, F. C. (1995). Distance metrics on the rigid-body motions with applications to mechanism design. *Journal of Mechanical Design*, 117(1):48–54.

Rublee, E., Rabaud, V., Konolige, K., and Bradski, G. (2011). Orb: An efficient alternative to sift or surf. In *Proceedings of the 2011 International Conference on*

Computer Vision, ICCV '11, pages 2564–2571, Washington, DC, USA. IEEE Computer Society.

Schmalstieg, D., Fuhrmann, A., Hesina, G., Szalavári, Z., Encarnaçao, L. M., Gervautz, M., and Purgathofer, W. (2002). The Studierstube augmented reality project. *Presence: Teleoperators and Virtual Environments*, 11(1):33–54.

Smeulders, A. W., Chu, D. M., Cucchiara, R., Calderara, S., Dehghan, A., and Shah, M. (2014). Visual tracking: An experimental survey. *Pattern Analysis and Machine Intelligence, IEEE Transactions on*, 36(7):1442–1468.

Tank, T. and Linnartz, J.-P. (1997). Vehicle-to-vehicle communications for avcs platooning. *IEEE Transactions on Vehicular Technology*, 46(2):528–536.

Winkens, C., Fuchs, C., Neuhaus, F., and Paulus, D. (2015). Optical truck tracking for autonomous platooning. In Azzopardi, G. and Petkov, N., editors, *Computer Analysis of Images and Patterns: 16th International Conference, CAIP 2015, Valletta, Malta*, volume 9257 of *LNCS*, pages 38–48, Cham. Springer.

Wu, Y., Lim, J., and Yang, M.-H. (2015). Object tracking benchmark. *Pattern Analysis and Machine Intelligence, IEEE Transactions on*, 37(9):1834–1848.

yves Bouguet, J. (2000). Pyramidal implementation of the lucas kanade feature tracker. *Intel Corporation, Microprocessor Research Labs*.

Zhu, G., Porikli, F., and Li, H. (2015). Tracking randomly moving objects on edge box proposals. *arXiv preprint arXiv:1507.08085*.